JJBS

Volume 18, Number 2,June 2025
ISSN 1995-6673
Pages 281 – 290
https://doi.org/10.54319/jjbs/180209

Jordan Journal of Biological Sciences

Preparation and Characterization of *Newbouldia laevis* (P.Beauv.) Seem. mediated Gold and Alloy Nanoparticles and Evaluation of Its Bactericidal Effect on Clinical Pathogens

Oluwakemi Abike Thonda[1,*], Fatimah Adenike Ajadi[2], Olanrewaju Oludotun Daramola[3], Aderiike Adewumi Grace[4], Oludare Temitope Osuntokun[5], Daniel Ayandiran Aina[1], Temitope Elizabeth Oyewole[1], Rukevwe Collins Etareri[1]

[1] Department of Microbiology, School of Science and Technology, Babcock University, Ilishan- Remo, Ogun State, Nigeria; [2]Department of Microbiology, Faculty of Sciences, Federal University of Health Sciences, Ila Orangun, P.M.B 204, Osun Nigeria; [3]Department of Physics, Lead City University, Ibadan, Nigeria; [4]Department of Basic Sciences, School of Science and Technology, Babcock University, Ogun State, Nigeria; [5]Department of Microbiology, Faculty of Science, Adekunle Ajasin University, Akungba Akoko. Ondo State Nigeria.

Received: July 5, 2024; Revised: September 25, 2024; Accepted: November 7, 2024

Abstract

Green synthesized nanoparticles using medicinal plants has become optimistic which can overcome the challenges of antimicrobial resistance while also providing additional benefits, such as cost-effectiveness and sustainability. The study, therefore, seeks to synthesize gold and alloy nanoparticles using *Newbouldia laevis* (P.Beauv.) Seem extracts and investigate their anti-bacterial property against multidrug pathogenic bacterial strains. The characterization of the nanoparticles synthesized was carried out using Ultra violet visible spectroscopy, fourier transform infrared spectroscopy, scanning and transmission electron microscope, energy dispersive analysis, and X-ray diffractive. The antibiotic susceptibility of the test organism and anti-bacterial effects of the synthesized nanoparticles were evaluated using disc diffusion and agar-well diffusion method, respectively. The absorbance peak results of the gold and alloy nanoparticles range between 228 - 530 nm, while the band gap of each is at 3.46 eV and 3.52 eV, respectively. The gold and alloy nanoparticles showed almost similar functional groups which ranged between 464.90 cm^{-1} and 3426.25 cm^{-1}. The shape of the synthesized nanoparticles was spherical, and the average particle size was 34.61 nm and 79.86 ± 32.11 nm, respectively. The gold and alloy nanoparticles inhibited the organisms at varying levels. The gold nanoparticles highest zone of inhibition was 23.5 mm against *Pseudomonas aeruginosa*, while alloy nanoparticle was 20 mm against *Staphylococcus aureus*. The synthesized gold and alloy nanoparticles using *Newbouldia laevis* extract showed increased sensitivity rate against the multidrug resistance organisms, which can be related to the presence of functional groups and bioactive compounds. This may be useful in various clinical applications, may reduce the resistance of these bacteria to antibiotics, and may be used as drug delivery systems.

Keywords: Alloy-*Newbouldia laevis*, Bactericidal effect, Green synthesis, Medicinal plant, *Newbouldia laevis*, *Newbouldia laevis*-nanoparticles.

1. Introduction

Since the use of plants to make herbal drugs combinations, it has greatly improved human health and their wellbeing, these plants have historically offered hope and life for new therapeutic substances. Ascorbic acid, phenols, citric acid, polyphenols, flavonoids, alkaloids, and terpenoids are the main classes of bioactive substances found and present in plants. (Timoszyk, 2018; Stozhko et al., 2019). Numerous substances under these categories of compounds possess antioxidant activities as well as the capacity to convert gold ions into metallic gold (Sathishkumar et al., 2018). It has been demonstrated that a variety of secondary metabolites present in plants, such as flavonoids, alkaloids, terpenoids, and tannins, have anti-microbial properties *in-vitro* and are abundant in plants (Singh et al., 2016). *Newbouldia laevis* (*N. laevis*) often refers to as the "Tree of Life" or boundary-tree, and is one of the magical plants (Byrappa et al., 2008). *N. laevis* is a growing plant with a height of approximately 7-8 (up to 15) meters. *N. laevis* is an average-sized angiosperm that is a member of the Bignoniaceae family. Searching for substances which possess antimicrobials and property in plants and plant parts are necessary because of their wide spread usage in treatments of variety of infections, infectious diseases and health-related problems. *Newbouldia laevis* is a plant that is frequently planted as an ornamental. Its leaves are glossy and dark-green in colour, enormous, spectacular purple-lilac blooms, and can be easily planted and replicated. Essentially, it is a symbolic or sacred tree that is planted effectively as a fence and frequently allowed to spread into a stockade. The stem, the fruits, and the leaves have been used as a

* Corresponding author. e-mail: thondao@babcock.edu.ng .

febrifuge for dressing of wound, and as a medicine for stomachaches (Iwu, 2000). It has been scientifically reported that *N. laevis* have medicinal value which ranged from anti-inflammatory to anti-oxidant, anti-microbial, anti-fungi, pain-killer and wound healing properties (Makarov et al., 2014; Omeje et al., 2020). To be precise, it has been claimed that combining stem bark with clay and red pepper can effectively treat many illnesses, such as bone lesions, and prevent pneumonia, fever, colds, and cough (Byrappa et al., 2008). In Africa, traditional medicine frequently used *N. laevis* to cure certain conditions like coughs and cold, toothaches, malaria, fever, stomachaches, STDs, constipation and breast cancer, eye problems and dysentry (Arbonnier, 2004; Ugwoke et al., 2024).

There are several names for *N. laevis*, often known as the boundry tree which is the common name, including Aduruku (Hausa), Ogirisi (Igbo), and Akoko (Yoruba). According to Usman and Osuji (2007), the bark is chewed and consumed in Nigeria to treat toothaches, diarrhea, and stomachaches. Swollen legs (Elephantiasis), syphilis, dysentry, rheumatism swellings, constipation, piles, and roundworms have all been successfully treated with the plant. According to Usman and Osuji (2007), boundry tree has also been reported to be helpful for chest discomfort, epilepsy, earaches, aching feet, and convulsions in youngsters. People have used the fruits, leaves, and stem as remedies for stomachaches, wounds, fevers, and other ailments (Obum-Nnadi, et al., 2020). Plants play important roles in our daily activities, right from the use of plants as food, such as vegetables, to their use as medicine for treating infections and in post-harvest storage of some agro commodities for security purposes. The plant is used to cure septic wounds and eye infections in parts of South Eastern and Midwestern Nigeria (Usman and Osuji, 2007). Obum-Nnadi et al. (2020) reported in their research findings the phytochemical and active compounds present in plants to be alkaloids and phenyl propanoids detected in the root, flavonoids, and tannins found in the leaf. Additionally, *N. laevis* is rich in diverse bioactive compounds, including tannins, terpenoids, and flavonoids, making it an ideal candidate for addressing the global issue of Antimicrobial Resistance (AMR). Furthermore, *N. laevis* has a wealth of different bioactive substances, such as flavonoids, terpenoids, and tannins, which makes it an excellent option for combating the global challenge of antimicrobial resistance (AMR).

Green synthesis that uses bacteria, fungus, plants, actinomycetes, algae, and other microorganisms, may be used as a cost-effective, environmentally benign, and a biocompatible method (Sathishkumar et al., 2018; Bachheti et al., 2020; Riaz et al., 2023). During green synthesis, several of phytochemical compounds, such as alkaloids, terpenoids, and phenolics assist in lowering and stabilizing metal ions (Khanna et al., 2019). A quite number of researchers have investigated the synthesis of metallic nanoparticles such as alloys, silver, and gold using various plant parts like leaves and barks. Thirumurugan et al. (2010) reported the synthesis of gold-nanoparticles using the *Azadirachta indica* plant, while Singh and Kochhar (2012) reported the production of gold nanoparticles using extracts from the leaves and bark of *Ficus carica*. Gold nanoparticles (AuNP) have been used as laboratory tracers in DNA finger-printing to find the presence of DNA in samples and immune-chemical experiments for protein interactions discovery. Additionally, they have been used to identify aminoglycoside drugs including gentamycin, neomycin, and streptomycin. In order to diagnose cancer and distinguish different bacterial groups, gold nanorods are essential for detecting cancer stem cells (Tomar *et al.*, 2013). The alloy nanoparticles' structural characteristics are different from those of their bulk counterparts. Bimetallic alloy nanoparticles, in particular, showed advantages above regular metallic nanoparticles (Mohl *et al*., 2011). According to Sánchez-López et al. (2020), metallic nanoparticles have demonstrated efficacy against a varieties of infections as well as selectivity for specific bacterial strains. Furthermore, to combat antibiotic resistance and boost the effectiveness of antibiotics, metallic nanoparticles have been used in combination with them (Allahverdiyev et al., 2011; Ghasemi and Jalal, 2016). Different nanoparticles suppress pathogens by different ways; for example, metallic NPs particularly have been revealed to penetrate cell walls of bacteria and form pores on the surface of the membranes, which results in creation of free radicals that damage the cell membrane (Acharya et al., 2023).

Plants generally have been reported and identified to be a huge source of novel drug compounds, which has contributed to human health and wellbeing. Plants such as *N. leavis* are rich in varieties of bioactive compounds such as tannins, terpenoids, flavonoids and many more. Scientific reports on the phytochemical constituent of the plants make it a better drug candidate. However, antimicrobial resistance (AMR) today is a major global problem that needs urgent attention as to find alternative therapy and research for novel drug candidate that can be used to tackle AMR. However, the goal of this study was to examine the characterization of *N. leavis* mediated gold and alloy nanoparticles and to determine their anti-microbial properties against pathogenic microorganisms of clinical importance.

2. Materials and Methods

2.1. Sample Collection and Organisms

Fresh *N. laevis* leaf sample were obtained from Ilishan-Remo Ogun State, Nigeria; they were identified by plant taxonomist and authenticated in the Department of Botany, University of Ibadan, Oyo State, Nigeria. The culture media used for culturing the isolates were MacConkey agar, Mannitol salt agar and nutrient agar (Himedia Laboratories Pvt. Ltd., Mumbai, India). The clinical isolates such as *Pseudomonas aeruginosa (P. aeruginosa*), *Escherichia coli* (*E. coli*), *Proteus vulgaris* (*P. vulgaris*), *Listeria monocytogenes* (*L. monocytogenes*), and *Staphylococcus aureus* (*S. aureus*) used as test organisms for gold and alloy nanoparticles were multidrug resistance pathogens and obtained from Microbiology Department, Babcock University, Ilishan, Ogun State, Nigeria.

2.2. Preparation of Newbouldia laevis extract

Aqueous extraction of the samples was prepared according to Aina *et al.*, 2018. Briefly, the plants were air dried at room temperature, and pulverized into fine powder. Five (5 grams) of the powdered samples was dispensed in 50 ml of distilled water and heated in the

water bath for twenty minutes. The solution was allowed to cool and filtered (Whatman filter paper No. 1); centrifugation was done at 4000 rpm for fifteen minutes. The supernatant was collected inside bottle and kept for further analysis and was used for the synthesis of the NP.

2.3. Preparation of 1 mM Gold and 1 mM Alloy

Approximately, 0.2589g of tetrachloroauric(III)acid trihydrate ($HAuCl_4 \cdot 3H_2O$) and silver nitrate ($AgNO_3$) (0.1699g) were dissolved in 1000ml of water to obtain 1 mM concentrations of gold and silver, respectively**.** The preparation of the alloy was done at 50:50 mixture ratio of silver and gold salts.

2.4. Preparation and Confirmation of organisms

The test organisms were collected and were resuscitated by sub-culturing on macConkey agar and nutrient agar. The organisms were inoculated by using four quadrant streaking method, followed by incubation at 37℃ for 18 hours. They were re-identified to confirm the identity using standard methods according to Thonda et al. (2020). The test organisms were standardized following 0.5 McFarland's standard ($x10^8$CFU/ml) using the spectrophotometer at 600 nm; the test organisms were then introduced into 2 ml of normal saline in a test tube to maintain bacterial activity by controlling the turbidity of the suspension. Each test tube was labelled according to the name of the organism.

2.5. Synthesis of Gold and Alloy nanoparticles

The biological synthesis of (gold and alloy) nanoparticles with *N. laevis* was done by introducing approximately 1 ml of the extract to each of the reaction vessels which contains forty milliliters (40 ml) of 1 mM gold and alloy solution respectively. Under static conditions, the reaction was carried out at room temperature (37 ℃ for 2 hours). The solutions were then put under sunlight for 30 minutes after thorough shaking to obtain visible colour change.

2.6. Characterization of N. laevis synthesized Gold and Alloy Nanoparticles

The UV-visible analysis of the NP was carried out using Shimadzu UV-visible (UV-1650PC) spectrophotometer with scan between 200 and 800 nm. The vibrational frequencies of the nanoparticles were determined through Fourier Transform Infrared Spectroscopy (FTIR) (model 84005 Shimadzu, Japan) transmission spectra by potassium bromide (KBr) as described by Liaqat *et al*. (2022). Fourier transform infrared spectroscopy analysis was carried out to identify the functional group present that assists in the synthesis of NP. The synthesized NP were further characterized using Scanning Electron Microscope (SEM) to determine the shape of the nanoparticles. Transmission Electron Microscope (TEM) was used for imaging and analytical characterization of the nanoparticles size and morphology and distribution of the NP, while Electron Diffractive X-ray analysis (EDX) analysis was conducted to identify the composition of elements of the synthesized nanoparticles present, and X-ray diffraction (XRD) analysis was carried out to analyze the crystalinity of the NP. The results were recorded (Varadavenkatesan et al., 2021; Oyewole et al., 2023).

2.7. Antibiotic Sensitivity Testing of the test organisms

The susceptibility testing of the test organisms was evaluated using Kirby - bauer disk diffusion methods (Thonda et al., 2021; Bale et al. 2022). The array of antibiotics and its concentration used were gentamycin (10 µg), augmentin (30 µg), ofloxacin (5 µg), ceftazidime (30 µg), cefixime (30 µg), ciprofloxacin (5 µg). nitrofurantoin (300 µg), and ceftriazone (30 µg). Briefly, the test organisms were standardized and inoculated by streaking onto Mueller Hinton agar plates; they were allowed to diffuse after the antibiotic disk was then placed gently on the plates. Incubation of the plates was done in an inverted position at 37 ℃ for 24 hours. The resultant zone diameter of inhibition was measured and recorded.

2.8. Antimicrobial activities assay of N. laevis gold and alloy synthesized nanoparticles

Determination of antimicrobial activities of the gold nanoparticles (AuNP-NL), and alloy nanoparticles (AlloyNP-NL), was carried out using agar well diffusion method. The NP gradient concentrations were prepared at various concentrations ranging from 10-100 µg/ml. Approximately, 750 ml of Mueller Hinton agar was prepared following the manufacturer's instruction; the media was dispensed into petri dishes and allowed to set. Each petri dish was labelled appropriately with gradient concentrations and control. Then, the test organisms were standardized following the McFarland standard; the standardized organisms were spread using a swab stick. A sterile cork borer (6 mm) was used to aseptically bore wells on each plate and appropriately labeled. A sterile micropipette was used to introduce approximately 0.1 ml each of the various concentrations of the synthesized AuNP-NL and AlloyNP-NL, including the control, into the bored holes. The incubation of plates were done at 37 ℃ for 24 hours (Oyewole et al., 2023). After incubation, the inhibition zone was examined and measured using a measuring ruler and the values were recorded in triplicates appropriately. These measurements were considered as the zone diameter of inhibition of the nanoparticles under investigation at different concentrations. Minimum inhibitory concentration and minimum bactericidal concentrations were determined using agar well diffusion method (Coyle 2005; Thonda et al., 2021).

3. Results and Discussion

Visual observation of the gold and alloy NP is depicted in Figure 2. Gold nanoparticles colour initially changed visually from colourless to light yellow and then changed to dark violet on addition of *N. laevis* extract as shown in figure 2a while alloy NP colour changed visually from colourless to dark purple on the addition of *N. laevis* extract, which acted as a reducing agent (Figure 2b). The colour changes that were obtained in the experiment indicated the formation of the respective nanoparticles. The colour variations observed in the solution indicated the presence of both gold and alloy NP, attributed to the activation of surface plasmon vibrations. The rapid consumption of reactants led to the generation of smaller nanoparticles. The absorbance peaks for the gold nanoparticles was observed at 301.25 nm at UV region and 530.72 nm at visible light region (Figure 3a). The formation of AuNP-NL was ascertained by the detection of

surface plasmon resonance (SPR) peak in UV–visible spectra analysis at 530nm resulting in the peak intensity which fall within limits (500 nm-600 nm). This maybe a result of surface plasmon resonance (SPR) features of gold nanoparticles. It has been reported that the colour variation in AuNP is thus due to the SPR features, which is dependent on the concentration, size, and shape of the NPs (He and Lu, 2018). The results of those findings are similar to the report of Dharman et al. (2023) who observed a dark yellow to dark greenish-yellow colour using cucurmin extract for the gold nanoparticles synthesis of with absorption peak at 530 nm which is a result of the excitation of the SPR (Dharman et al., 2023). The band gap was obtained at 3.46 eV as depicted in figure 3b. In figure 4a, the alloy nanoparticles (AlloyNP-NL) spectrum had peaks absorbance at 228.41 nm and 310.19 nm at the UV region and 529.57 nm at visible light region. The alloy NP band gap was obtained at 3.52 eV as shown in figure 4b. This is in line with the study of Fouda et al., (2022) who observed absorbance peak at 530 nm. Maliszewska et al. (2021) observed a single plasmon (SPR) band at 522 – 523 nm and reported that a single SPR peak appeareing at a λmax in the 520–540 nm region indicated the creation of tiny, spherical, and monodispersed AuNPs (Muddapur et al., 2022).

Figure 1: Visual observation of NP before and after exposure to sunlight (A) Gold nanoparticles before and after (B) Alloy nanoparticles before and after being synthesized with *Newbouldia laevis.*

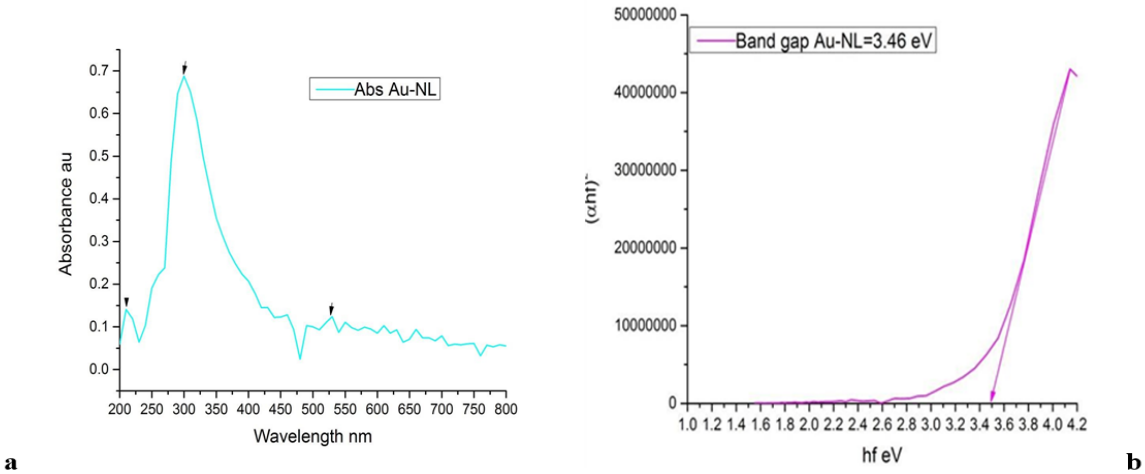

Figure 2: (a) UV-Vis Spectra of AuNp-NL showing the absorbance peak (b) Band gap of AuNp-NL showing at 3.46 eV

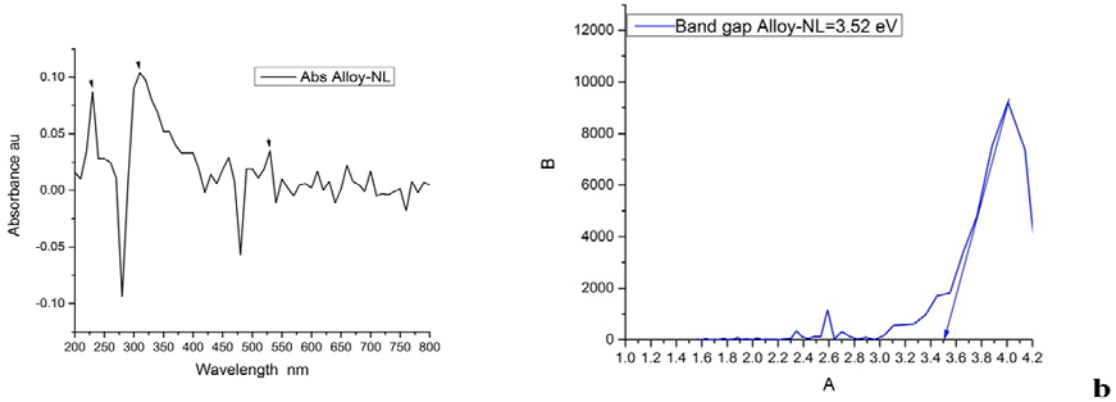

Figure 3: (a) UV-Vis Spectra of AlloyNp-NL showing the absorbance peak (b) Band gap of AlloyNps-NL showing at 3.52 eV

The FTIR analysis of the gold and alloy mediated nanoparticles *N. laevis* is depicted in Figure 5. The gold and alloy showed minimum absorbance peak at 464.90cm^{-1} and 470.96cm^{-1} respectively. However, the maximum absorbance peaks observed for gold nanoparticles was 3426.25cm^{-1} and 3419.33cm^{-1} for alloy nanoparticles in FTIR spectrum respectively. The gold NP showed 12 peak values while alloy nanoparticles showed 17 peak values (Figure 5). The extract's functional groups for the synthesized nanoparticles were identified using FTIR. Gold and the alloy nanoparticles investigated showed the same functional groups of Oxide of metal, Polysulfides (S-S stretch), -C-O-C- vibration, Secondary alcohol C-O stretch, gem-Dimethyl or ‘‘iso’’- (doublet), Methyl C-H asym./sym. Bend, CH stretching Vibration, methyne C-H stretch Symmetric CH_3 Stretch and –OH stretch. Whereas different functional groups detected in gold NPs are indicated at 659.62 cm^{-1} (aliphatic bromo compounds) and at 1626.25 cm^{-1} (C-Br stretch, Alkenyl C=C stretch). *N. leavis* has been reported to have some functional groups of compounds in which the peak ranges from 756.12cm^{-1} to 3448.84 cm^{-1}. The functional groups are: polychlorinated (C-Cl str.), nitramines (C-N vib.), secondary alcohol (C-O str.), tertiary alcohol (O-H Def.), secondary alcohol (O-H def.), alkanes (C-H def.), Nitrosamines (N=O str.), amino acid ($NH3^{+}$def.), ketones (C=O str.) and ketones (C=O overtone; C=O str.) (Omeje et al., 2020). Some functional groups such as secondary alcohol and alkanes were present in both *N. leavis* extract and the synthesized NP. Similarly, different functional groups were found for alloy at 907.98 cm^{-1} (Vinyl C-H out of plane bend) and at 1572.60 cm^{-1} (Secondary amine, >N-H bend) respectively. As a result of the presence of bioactive phytochemicals in the *N. laevis*, leaves extract such as alkaloids flavonoids, and tannins as revealed by Obum-Nnadi, et al. (2020) has the capacity to convert gold and alloy into NP and stabilize the products. A broad peak in the range of 3426 to 3419 cm^{-1} was identified as O-H vibrations and or N-H stretches associated with N-substitute amide in this study. Aina *et al*. (2018) also reported the same peak as O-H stretch. The peaks at 2426 cm^{-1} and 2360 cm^{-1} were attributed to atmospheric carbondioxide (CO_2) absorption, suggesting that the nanoparticles possess CO_2 absorption capabilities. Furthermore, the 1384 cm^{-1} peak was linked with C-H in plane bending of alkenes and aromatics. The presence of these characteristic peaks confirmed the successful encapsulation of certain biomolecules, such as proteins and carbohydrates from *N. laevis* on the synthesized nanoparticles.

The gold and alloy nanoparticles shapes (Figure 6) were characterized using SEM. The results revealed the spherical polydispersed shape of AuNP-NL and AlloyNP-NL. The TEM image used to analyze the size distribution and average particle size of the NP is shown in Figure 7. The sizes of the particle vary from 15 to 60 nm, with the majority of particles for AuNP-NL falling between 35 and 40 nm in size. The average particle size of AuNP-NL was 34.61 nm in size (Figure 7A), while the average particle size of the AlloyNP-NL and its standard deviation was 79.86 ± 32.11 nm (Figure 7B). The size of the gold NP is comparable to the study of Tao et al. (2019), which found that the nanoparticles were spherical in shape and highly crystalline in nature; AuNPs with particle sizes of 20–60 nm were prepared and thereby reduced $HAuCl_4$ using aqueous extract of *aloe-vera* leaves while the extract was being protected. AuNPs were also found to have good stability and to be less prone to oxidation and agglomeration. The size of the NPs reported in this study is in line with the report of Huang et al. (2019) who found that the average particle sizes of AuNPs produced using the *Dillenia indica* aqueous leave extract ranged from 5 to 50 nm, while those formed using *Garcinia mangostana* aqueous extracts peel and *Mentha longifolia* leaves were 32.9 ± 5.3 nm and 36.4 nm, respectively (Lee et al., 2016; Li et al., 2021). The secondary metabolites identified from plants varied between the plants and are utilized as stabilizing, capping, and reducing agents which may be responsible for the variance in particle sizes.

Element dispersive (EDS) analysis of AuNP-NL and AlloyNP-NL synthesized from *N. laevis* is depicted in Figure 8. Signals of Gold were found in AuNP-NL at 74.72 weight % along with other elements of C (4.50 wt. %) and O (20.68 wt. %) with composition percentage which showed the purity of the synthesized AuNP-NL (Figure 8a). However, the alloyNP-NL showed Au element in 75.56 wt. % along with other elements of C, Fe, O and Na with 5.34, 7.40, 13.37 and 3.30 wt. % respectively. It was noticed that Au content was in higher percentage in the AuNP-NL and AlloyNP-NL (Figure 8b). The signals from the other elements in the EDS could be the result of compounds that are partially or fully bound to the alloyNP and AuNPs. The corresponding XRD patterns of the NP are presented in Figure 8c and 8d. Gold nanoparticles and AlloyNP-NL exhibited the same five distinct peaks at 2θ. All five peaks attributed to crystallographic planes corresponded to standard Bragg reflections (110), (111), (121), (200) and (311) of the face center cubic (fcc) lattice plan according to JCPDS files. The crystalline form of the *N. laevis* nanoparticles is confirmed by the observation of distinctive Bragg diffraction peaks (Kratosova et al., 2013).

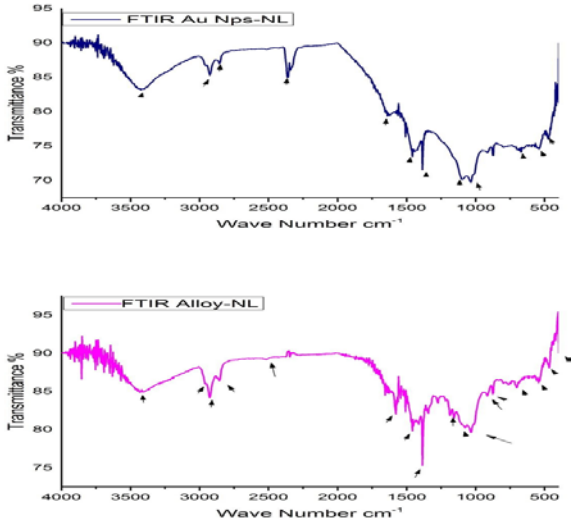

Figure 4: FTIR spectra for AuNP-NL and AlloyNP-NL synthesized nanoparticles

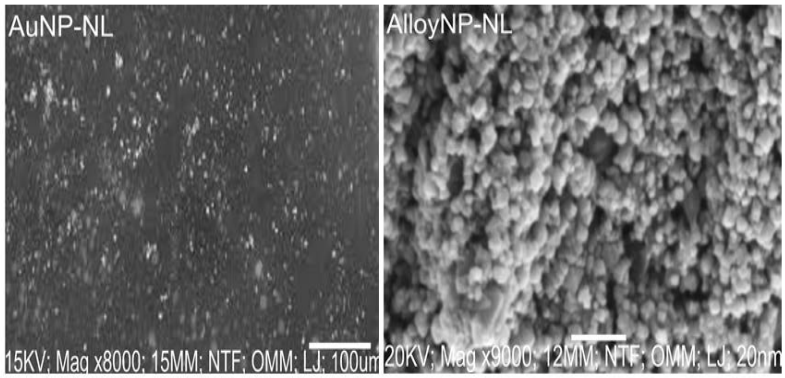

Figure 5: SEM Images of *N. laevis* mediated gold and alloy NP

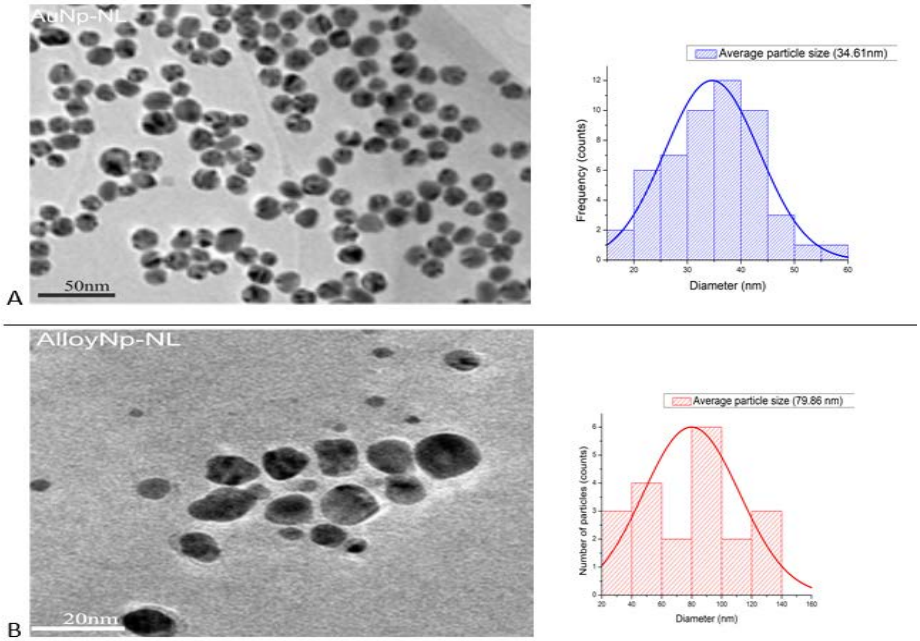

Figure 6: TEM Images and Histogram distribution of the Particles Size (A) AuNP-NL (B) AlloyNP-NL

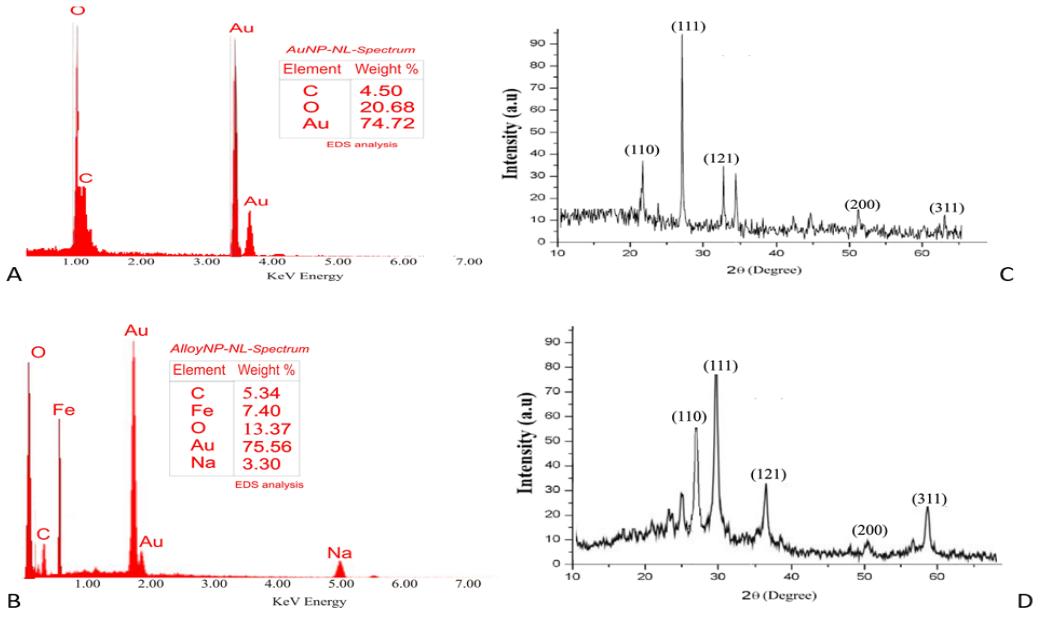

Figure 7: EDS analysis of AuNP-NL (A), AlloyNP-NL (B) and XRD spectra of AuNP-NL (C), AlloyNP-NL (D) synthesized from *N. laevis*

The evaluation of the antibiotic sensitivity test was carried out on the organisms (*P. aeruginosa*, *P. vulgaris*, *E. coli*, *L. monocytogenes* and *S. aureus*) as depicted in Figure 9. The zones of inhibition of each organisms were measured in millimetre (mm). The results showed that all the test organisms were 100% resistant to augmentin, ceftazidime, cefixime and ceftriaxone; they showed no inhibition zones against all tested bacterial strains, while the organisms showed 40% resistant to nitrofurantoin. However, they are 100% susceptible to gentamicin, ofloxacin and ciprofloxacin (Figure 9). The effectiveness of commercially used antibiotics varied across different bacterial strains, indicating the importance of choosing appropriate antibiotics based on bacterial susceptibility profiles to ensure effective treatment. Additionally, the data underscores the emergence of antibiotic resistance in certain bacterial strains, highlighting the reason for judicious antibiotic use and the development of possible alternative treatment strategies.

The evaluation of anti-bacterial activities of AuNP-NL, AlloyNP-NL, positive and negative control, was examined against test organisms namely *P. aeruginosa*, *P. vulgaris*, *E. coli*, *L. monocytogenes* and *S. aureus*. The zones of inhibition (mm) are represented in Tables 1 and 2 respectively. There was no inhibition zone (anti-bacterial activity) observed at concentrations of 10 µg/ml and 20 µg/ml (the lowest concentrations) as well as the negative control (water) for all tested organisms. The organisms were sensitive to ciprofloxacin antibiotics (positive control) as it showed inhibitory zones ranging from 15.5 mm and 26 mm. Zones of inhibition were observed at 40 µg/ml for all strains, except *P. vulgaris*, which showed no activity at 40 µg/ml (Table 1). The synthesized nanoparticles are concentration-dependent as there is a clear trend of increasing antibacterial activity with increase in concentration. The AuNP was more effective at higher concentration as compared to ciprofloxacin. All bacterial strains showed maximum zones of inhibition at the highest concentration tested (100 µg/ml). The higher the concentration is, the better is the activity of the synthesized nanoparticles. The anti-bacterial activity of the alloy nanoparticles against test organisms is presented in Table 2. The Alloy-NP exhibit significant antibacterial activities especially at higher concentrations as compared to the negative control as compared to the positive control which showed wide zones of inhibition against all the organisms. *P. aeruginosa* and *P. vulgaris* exhibited inhibition zones only at higher concentrations (60 µg/ml and above). *Staphylococcus aureus* showed an irregular inhibition pattern, but significant inhibition was at higher concentration. *E. coli* and *L. monocytogenes* showed a consistent increase in inhibition zones from 40 µg/ml. There was no activity for synthesized alloy nanoparticles at 10 µg/ml and 20 µg/ml; No inhibition zone against *P. aeruginosa* and *P. vulgaris* at 40 µg/ml as shown in Table 3. As the concentrations of alloy nanoparticles increased, the antibacterial activities also increased. These nanoparticles could be promising candidates for treating infections, particularly those caused by resistant strains. The Minimum Inhibitory Concentration (MIC) of AuNP-NL and AlloyNP-NL was determined at concentrations 100, 50, 25, 12.5, 6.25 and 3.12 mg/ml. The results showed that the organisms were inhibited at concentrations 100, 50.0 25.0 and 12.5. The MIC of the gold and alloy nanoparticles was 50 and 25 mg/ml respectively, which indicated that nanoparticles are effective at higher concentrations. The minimum bactericidal concentration of both alloy and gold NP was recorded at 25 mg/ml.

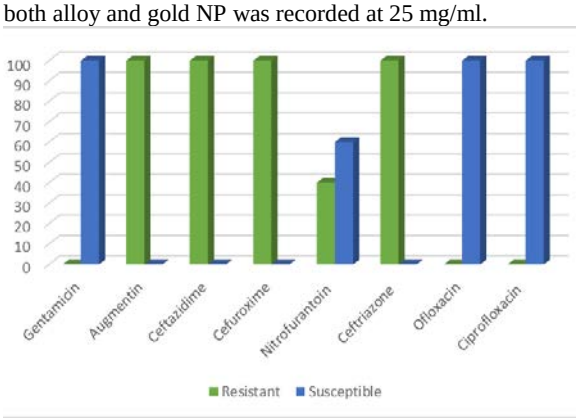

Figure 8: Antibiotic Susceptibility of the test organisms using disk diffusion method

Table 1: Antibacterial activity of synthesized AuNp-NL against test organisms using agar well diffusion method

Concentration	Ciprofloxacin (10µg)	Water	10	20	40	60	80	100
	Zones of inhibition (mm)							
Escherichia coli	15.5	0	0	0	8	10.5	12.5	18
L. monocytogenes	21	0	0	0	8.5	9.5	12.5	19
P. aeruginosa	23	0	0	0	10.5	11.5	15	23.5
P. vulgaris	26	0	0	0	0	10.5	12.5	17
S. aureus	25	0	0	0	8.5	9	12.5	21

Key: Concentrations are in µg/ml

Table 2: Zones of inhibition obtained from the synthesized AlloyNP-NL against pathogenic organisms using agar well diffusion method

Concentration	Ciprofloxacin (10 µg)	Water	10	20	40	60	80	100
	Zones of inhibition (mm)							
Escherichia coli	15.5	0	0	0	9	11.5	13.5	14
L. monocytogenes	21	0	0	0	7.5	10.5	13.5	14
P. aeruginosa	19	0	0	0	0	10.5	15.5	16.5
P. vulgaris	22.5	0	0	0	0	12.5	13.5	14
S. aureus	23	0	0	0	10.5	08	13.5	20

Key: Concentrations are in µg/ml

Medicinal plants are efficient remedies for a variety of disorders and conditions because they are easily available, cost effective, reliable, and have few to no adverse effects. Plants create bioactive or secondary chemicals as a defense strategy to ward off pests, attract pollinators, and aid in the survival of the species. There have been reports of medical benefits for *N. laevis*, including analgesic, anti-inflammatory, antioxidant, wound healing properties, antibacterial, and anti-fungal qualities (Akerele et al., 2011; Akande et al., 2020). The bark has traditionally been used to treat skin infections, Diarrhoea, tooth aches, stomach aches, fever, and other ailments are treated with a decoction of the bark. The present investigation revealed that the use of *N. laevis* in green synthesis facilitated the reduction of $HAuCl_4$ salt, thus, leading to the formation of

NP in just thirty minutes with the evidence of colour change. This supports the findings of Zangeneh and Zangeneh (2020) which showed that aqueous extract from *Hibiscus sabdariffa* flowers decreased $HAuCl_4 \cdot 3H_2O$ and produced spherical gold nanoparticles with a 15–45 nm particles size. To accomplish the green synthesis of AuNPs, *N. laevis* can be utilized as stabilizing and reducing agents and $HAuCl_4$ as the precursor. There have also been reports of the synthesis of AuNPs utilizing *Camellia sinensis* (green tea) extract as a reducing and stabilizing agent (Vilchis-Nestor et al., 2008).

This research showed that the gold and alloy nanoparticles have antibacterial activity against the test organisms which were able to inhibit all the organisms (*P. vulgaris, L. monocytogenes, P. aeruginosa, E. coli,* and *S. aureus*) at varying concentrations. From this study, it can be deduced that the antimicrobial activity of gold and alloy nanoparticles using *N. laevis* extract was high as compared to the control which showed no activity. The findings revealed that the alloy and gold nanoparticles exhibit potent antibacterial properties. This work is similar to that of Usman and Osuji (2007), who found that *N. leavis* extract had the broadest activity against the majority of the Gram negative pathogens they studied, including *Klebsiella* spp., *E. coli*, and *P. aeruginosa*. This further supports the results of Ayaz Ahmed et al. (2014), who found that gold nanoparticles made from the Indian plant *Salicornia brachiata* had strong antibacterial action against a number of pathogenic organisms, including *P. aeruginosa* and *E. coli* (Ayaz Ahmed et al. 2014). It was observed from this study that the higher the concentration, the more zones of inhibition obtained. This finding is consistent with the study by Fouda et al. (2022), which showed that the antibacterial efficacy of synthetic AuNP was contingent on dosage (dose-dependent). The findings of Muddapur et al. (2022) and Wani et al. (2013), which demonstrated that the anti-bacterial activity of biosynthesized NP depended on a number of variables, including concentration, size, and shape, are consistent with the findings of this study. The results of this study are in agreement with those of earlier reported studies (Inbaraj et al., 2020, Muniyappan et al., 2021). The main source of anti-bacterial activity is high surface to volume ratios, and the small size of nanoparticles facilitates their penetration of cell walls and membranes (Patil and Kim 2017; Wang et al., 2017). Using raw chemically produced AuNP, the dependence of antibacterial action on the size and concentration of AuNP was first confirmed and reported (Lavaee et al., 2021; Zhu et al., 2020). Numerous studies utilizing biosynthesized AuNP indicated that the stability, surface charge, and makeup of the AuNP envelope generated during the biological reduction process are the reasons for favorable antibacterial testing. These nanoparticles (gold and alloy) could be promising candidates for treating infections of those caused by the pathogenic strains.

4. Conclusion

The *N. laevis* mediated gold and alloy nanoparticles gotten from extract of exhibit significant and strong antibacterial properties against the pathogenic bacteria especially at higher concentrations which can be used as treating infections caused by these organisms. Higher concentrations are required for effective antibacterial activity, especially against multidrug resistant bacteria like *Pseudomonas aeruginosa* and *Proteus vulgaris*. Understanding the specific concentration thresholds for different bacteria is crucial for effective application. Further research into their mechanisms of action and potential clinical applications is warranted to fully explore their therapeutic potential.

Recommendations

1. Investigation into the mechanisms by which these gold and alloy nanoparticles *N. laevis* exert their antibacterial effects is necessary.
2. Additional studies could focus on optimizing nanoparticles synthesis and exploring their efficacy in clinical settings.

Authors Contribution

TOA and ADA conceptualized the experimental design and TOA, ERC, OTE, OOD performed the data analyses. ADA, TOA, OTE collected the samples. TOA, AFA, AAG, OOT wrote the manuscript. TOA, ERC and ADA performed the extraction and synthesize the nanoparticles. All authors contributed to the article and approved the final and submitted version.

References

Acharya B, Akansha R, Ashwani K, Shalini M, Vedpriya A, Vandana K, et al. 2023 Elucidating the Role of Plant Extracts Mediated Gold Nanoparticles as Smart Antimicrobials: Two-Way Attack, *J. Nanomaterials*, 4085090.

Aina AD, Owolo OD, Adeoye-Isijola MO, Aina FO, Omeiza F and Adewumi AG. 2018. Almond leaves for the one-pot Biofabrication of silver nanoparticles: Characterization and larvicidal application. *Int. J. Sci. Res. Pub*, **8 (11)**: 703-711.

Akande EB, Oladejo BO, Oladunmoye MK and Abodunrin TF. 2020. Antibacterial Effects of *Newbouldia laevis* {P. BEAUV} on the Bacteria Isolated from the Blood of Hepatitis C Virus Positive Individuals. *Asian Plant Res. J*, **4(1)**: 26-34.

Akerele JO, Ayinde BA and Ngiagah J. 2011. Phytochemical and antibacterial evaluations of the stem bark of *Newbouldia leavis* against isolates from infected wounds and eyes. *Trop J Pharm Res*, **10(2)**:211-218.

Allahverdiyev AM, Kon KV, Abamor ES, Bagirova M and Rafailovich M. 2011. Coping with antibiotic resistance: combining nanoparticles with antibiotics and other antimicrobial agents. *Expert Rev Anti Infect Ther*, **9(11)**: 1035-1052.

Arbonnier M. 2004 Trees, shrubs and lianas of West African dry zones. Cirad, Margraf, MNHN, 574 p.

Ayaz Ahmed KB, Subramanian S, Sivasubramanian A, Veerappan G and Veerappan A. 2014. Preparation of gold nanoparticles using Salicornia brachiata plant extract and evaluation of catalytic and antibacterial activity. *Spectrochim. Acta Part A Mol. Biomol. Spectrosc*, **130**: 54–58.

Bachheti RK, Fikadu, A, Bachheti A and Husen A. 2020. Biogenic fabrication of nanomaterials from flower-based chemical compounds, characterization and their various applications: a review. *Saudi J Biol Sci*, **27(10)**: 2551–2562.

Bale SI, Mukhtar MD and Rufa'i, FA. 2022. Bacteria Associated with Health-care Acquired infections from two Selected Hospitals in Kano, Nigeria. *Int. j. sci. res. biol. sci*, **9(4)**: 34-38.

Byrappa K, Ohara S and Adschiri T. 2008. Nanoparticles synthesis using supercritical fluid technology–towards biomedical application. *Adv. drug deliv. Rev*, **60(3):** 299-327.

Coyle MB. 2005. Manual of antimicrobial susceptibility testing. American Society for Microbiology (ASM) press, Washington, 39-62.

Dharman S, Maragathavalli G, Shanmugam R, Shanmugasundaram K. 2023. Curcumin mediated gold nanoparticles and analysis of its antioxidant, anti-inflammatory, antimicrobial activity against oral pathogens. *Pesqui Bras Odontopediatria Clín Integr*, **23:** e220068.

Fouda A, Eid AM, Guibal E, Hamza MF, Hassan SE-D and Alkhalifah DHM. 2022. Green Synthesis of Gold Nanoparticles by Aqueous Extract of *Zingiber officinale*: Characterization and Insight into Antimicrobial, Antioxidant, and In Vitro Cytotoxic Activities. *Appl. Sci*, ***12*:** 12879.

Gangwar RK, Tomar GB, Dhumale VA, Zinjarde S, Sharma RB and Datar S. 2013. Curcumin conjugated silica nanoparticles for improving bioavailability and its anticancer applications. *J Agric Food Chem*, **61(40)**: 9632-9637.

Ghasemi F and Jalal R. 2016. Antimicrobial action of zinc oxide nanoparticles in combination with ciprofloxacin and ceftazidime against multidrug-resistant *Acinetobacter baumannii*. *J Glob Antimicrob Resist*, **6:** 118–122.

He X and Lu H. 2014. Graphene-supported tunable extraordinary transmission. *Nanotechnology*, **25**: 325201. https://doi.org/10.1088/0957-4484/25/32/325201

Huang QH, Luo AH, Jiang LJ, Zhou Y, Yang YT, Liu Q and Zhang CF. 2019. Disinfection efficacy of green synthesized gold nanoparticles for medical disinfection applications. *Afr. Health Sci*, **19**: 1441–1448.

Inbaraj BS, Chen BY, Liao CW and Chen BH. 2020. Green synthesis, characterization and evaluation of catalytic and antibacterial activities of chitosan, glycol chitosan and poly (γ-glutamic acid) capped gold nanoparticles. *Int. J. Biol. Macromo,*. **161:**1484-1495.

Iwu MM. 2000. Handbook of African Medicinal Plants. London: CRC Press, Inc; p. 19.

Khanna P, Kaur A. and Goyal D. 2019. Algae-based metallic nanoparticles: synthesis, characterization and applications. *J Microbiol Methods*, **163**: 105656.

Kratošová G, Vávra I, Horska K, Životský O, Němcová Y, Bohunická M, Slabotinskú J, Rosenbergová K, Kadilak A and Schröfe A. 2013. Synthesis of metallic nanoparticles by diatoms and chrysophytes - prospects and applications. *Green Bio. Nano: Mec Appl*, 61-78. https://doi.org/10.1079/9781780642239.00

Lavaee F, Ranjbar Z, Modarezi F and Keshavarz F. 2021. The effect of gold nanoparticles with different sizes on *Streptococcus* species. *J. Dent.* **4:** 235–242.

Lee KX, Shameli K, Miyake M, Kuwano N, Khairudin NBBA, Mohamad SEB and Yew YP. 2016. Green synthesis of gold nanoparticles using aqueous extract of *Garcinia mangostana* fruit peels. *J. Nanomater*, **2016:** 8489094.

Li SQ, Al-Misned FA, El-Serehy HA and Yang, LL. 2021. Green synthesis of gold nanoparticles using aqueous extract of *Mentha Longifolia* leaf and investigation of its anti-human breast carcinoma properties in the in vitro condition. *Arab. J. Chem*, **14:** 102931.

Liaqat N, Jahan N, Rahman K, Anwar T. and Qureshi H. 2022. Green synthesized silver nanoparticles: optimization, characterization, antimicrobial activity and cytotoxicity study by hemolysis assay. *Front Chem*, **10:** 952006.

Makarov VV, Makarova SS, Love AJ, Sinitsyna OV, Dudnik AO, Yaminsky IV, Taliansky ME and Kalinina NO. 2014. Biosynthesis of stable iron oxide nanoparticles in aqueous extracts of Hordeum vulgare and Rumex acetosa plants. *Langmuir*, **30(20)**: 5982-8. doi: 10.1021/la5011924

Maliszewska I, Wanarska E, Thompson AC, Samuel IDW, Matczyszyn K. 2021. Biogenic gold nanoparticles decrease methylene blue photobleaching and enhance antimicrobial photodynamic therapy. *Molecules*, **26:** 623.

Mohl M, Dobo D, Kukovecz A, Konya Z, Kordas K, Wei J and Vajtai, R. 2011. Formation of CuPd and CuPt bimetallic nanotubes by galvanic replacement reaction. *J. Phys. Chem. C*, **115(19)**: 9403-9409.

Muddapur UM, Alshehri S, Ghoneim MM, Mahnashi MH, Alshahrani MA, Khan AA, Iqubal SMS, Bahafi A, More SS, Shaikh IA, Mannasaheb BA, Othman N, Maqbul MS, and Ahmad MZ.2022. Plant-based synthesis of gold nanoparticles and theranostic applications: A review. *Molecules*, **27(4):** 1391.

Muniyappan N, Pandeeswaran M and Amalraj A. 2021. Green synthesis of gold nanoparticles using Curcuma pseudomontana isolated curcumin: its characterization, antimicrobial, antioxidant and anti-inflammatory activities. *Environ Chem Ecotoxicol*, **3:** 117-124.

Obum-Nnadi CN, Okey-Ndeche FN, Nnagbo PA and Ohabughiro NB. 2020. Phytochemical and antibacterial activities of *Newbouldia laevis* leaves (ogirishi) on two drug resistant bacteria. *Int. J. Res. and Rev.* **7(5):** 59-66.

Omeje KO, Ezema BO, Ozioko JN, Omeje HC, Ogidigo JO, Okeke OR and Nnorom CO. 2020. Cholinesterases Inhibition and Antioxidant Potentials of *Newbouldia laevis* and *Ficus exasperata* Vahl Leaf Extract. *Archives*, **1:** 77-91

Oyewole TE, Thonda OA, Fagbemi KO and Amodu S. 2023. Comparative Study of Green Synthesis of Silver Nanoparticles Using Leaf Extracts of *Vitellaria Paradoxa* and Their Antioxidant Activities. *Cur. Trends Life Sci. Res*, **2(1):** 47-64.

Patil MP and Kim GD. 2017. Eco-friendly approach for nanoparticles synthesis and mechanism behind antibacterial activity of silver and anticancer activity of gold nanoparticles. *Appl. Microbiol. Biotechnol*, **101:** 79–92.

Riaz U, Anum W, Jatoi GH, Murtaza G, Qazi MA and Rehman M. 2023. Genetically modified organisms use in green synthesizes nanomaterials In: Ozturk, M., Roy, A., Bhat, R.A., Vardar

Sukan, F., Policarpo Tonelli, F.M. (eds.): Synthesis of Bionanomaterials for Biomedical Applications. Cambridge, *Elsevier*, pp. 151-163.

Sánchez-López E, Gomes D, Esteruelas G, Bonilla L, Lopez-Machado AL, Galindo R, Cano A, Espina M, Ettcheto M, Camins A, Silva AM, Durazzo A, Santini A, Garcia ML, Souto EB. 2020. Metal-based nanoparticles as antimicrobial agents: an overview. *Nanomaterials*, **10(2)**: 292.

Sathishkumar P, Gu FL, Zhan Q, Palvannan T and Yusof ARM. 2018. Flavonoids mediated 'green' nanomaterials: A novel nanomedicine system to treat various diseases. Current trends and future perspective. *Mater. Lett*, **210**: 26–30.

Singh J, Kaur G and Rawat M. A. 2016. Brief Review on Synthesis and Characterization of Copper Oxide Nanoparticles and its Applications. *J Bioelectron Nanotechnol*, **1(1)**: 9.

Singh, P.P. and Bhakat, C. 2012. Green Synthesis of Gold Nanoparticles and Silver Nanoparticles from Leaves and Bark of *Ficus carica* for Nanotechnological Applications. *Int. J. Sci. Res*, **2:** 1-4.

Stozhko NY, Bukharinova MA, Khamzina EI, Tarasov AV, Vidrevich MB and Brainina KZ. 2019. The effect of the antioxidant activity of plant extracts on the properties of gold nanoparticles. *Nanomaterials*, **9:** 1655.

Tao J, Fu Z, Dong C, Wang X, and Yang X. 2019. Green synthesis and characterization of monodisperse gold nanoparticles using aloe vera leaf extract. *Rare Metal Mat. Eng*, **48(11)**: 3470–3475

Thirumurugan A, Jiflin G, Rajagomathi G, Tomy N, Ramachandran S and Jaiganesh R. 2010. Biotechnological synthesis of gold nanoparticles of *Azadirachta indica* leaf extract". *Int J. Biol Tech*, **1**: 75-7.

Thonda OA, Okorie D, Ogidi CO, Aladejana OM, Olowookere BD and Olawoye AA. 2020. Antibacterial Efficacy of *Vernonia Amygdalina* Against Bacteria Strains Recovered from Hospital Fomites, Nigeria. *Curr Tr Biotech & Microbio.* **2(2)**: 381-388.

Thonda OA, Oluduro AO, Adewole OO and Obiajunwa PO. 2021. Phenotypic and genotypic characterization of plasmid-mediated AmpC beta-lactamases in enteric Gram-negative bacteria from patients with lower respiratory tract infections in a tertiary hospital, Southwest Nigeria. *Afr. J. Clin. Exp. Microbiol.* **22 (4):** 465–472.

Timoszyk A. 2018. A review of the biological synthesis of gold nanoparticles using fruit extracts: Scientific potential and application. *Bull. Mater. Sci*, **41:** 154–165.

Ugwoke HU, Ezema JN, Chinaka CB, Imanyikwa OE, Ukhureigbe OM, Ezugwu IA, Chukwuma ST and Eze EA. 2024. Evaluation of Antibacterial Effects of *Newbouldia laevis* and *Dracaena arborea* Methanol Extracts against Some Multidrug Resistant 'ESKAPE' Pathogens Isolated from Hospital Environments. *Trop J Nat Prod Res,* **8(7):** 7778-7785.

Usman H and Osuji JC. 2007. Phytochemical and in vitro antimicrobial assay of the leaf extract of *Newbouldia laevis. Afr J Tradit Complement Altern Med*, **4(4):** 476-80.

Varadavenkatesan T, Pai S, Vinayagam R and Selvaraj R. 2012. Characterization of silver nano-spheres synthesized using the extract of *Arachis hypogaea* nuts and their catalytic potential to degrade dyes. *Mater. Chem. Phys*, **272:** 125017.

Vilchis-Nestor AR, Sánchez-Mendieta V, Camacho-López MA, Gómez-Espinosa RM, Camacho-López MA and Arenas-Alatorre JA. 2008. Solventless synthesis and optical properties of Au and Ag nanoparticles using *Camellia sinensis* extract. *Mater. Lett*, **62:** 3103-3105.

Wang L, Hu C and Shao L. 2017. The antimicrobial activity of nanoparticles: Present situation and prospects for the future. *Int. J. Nanomed*, 1227–1249.

Wani IA and Ahmad T. 2013. Size and shape dependant antifungal activity of gold nanoparticles: A case study of Candida. *Colloids Surf. B-Biointerfaces*, **101:** 162–170.

Zangeneh MM and Zangeneh A. 2020. Novel green synthesis of *Hibiscus sabdariffa* flower extract conjugated gold nanoparticles with excellent anti-acute myeloid leukemia effect in comparison to daunorubicin in a leukemic rodent model. *Appl. Organomet. Chem*, **34(1):** 5271–5283.

Zhu S, Shen Y, Yu Y and Bai X. 2020. Synthesis of antibacterial gold nanoparticles with different particle sizes using chlorogenic acid. *R. Soc. Open Sci*, **7:** 191141–191151.